Carbohydrate Polymers 93 (2013) 709–717

Contents lists available at SciVerse ScienceDirect

Carbohydrate Polymers

journal homepage: www.elsevier.com/locate/carbpol

Physicochemical and antibacterial properties of surfactant mixtures with quaternized chitosan microgels

Kristopher E. Richardson[a], Zheng Xue[b], Yan Huang[a], Youngwoo Seo[a,b,c], Yakov Lapitsky[a,c,*]

[a] Department of Chemical and Environmental Engineering, University of Toledo, Toledo, OH 43606, United States
[b] Department of Civil Engineering, University of Toledo, Toledo, OH 43606, United States
[c] School of Green Chemistry and Engineering, University of Toledo, Toledo, OH 43606, United States

ARTICLE INFO

Article history:
Received 22 May 2012
Received in revised form 24 August 2012
Accepted 18 December 2012
Available online 27 December 2012

Keywords:
Surfactant
Chitosan
Antibacterial
Polyelectrolyte
HTCC
Microgels

ABSTRACT

Antibacterial surfactant mixtures attract widespread interest in the design of consumer product formulations, but often use toxic biocidal agents such as cationic surfactants, triclosan or bleach. To address this, we explored replacing these toxic ingredients with quaternized chitosan microgels, which combine high antibacterial activity with cytocompatibility with mammalian cells. Specifically, three essential properties of microgel mixtures with model anionic (sodium dodecyl sulfate, SDS) and nonionic (Triton X-100, TX-100) surfactants (and with SDS/TX-100 mixtures) were investigated: (1) colloidal stability, (2) antibacterial activity, and (3) hydrophobe solubilization. Additionally, the effect of surfactant on dispersion turbidity, which can be important in the formulation of aesthetically-appealing products, was explored. The microgels formed more-stable dispersions when mixed with nonionic TX-100, but quickly precipitated when mixed with the electrostatically-binding SDS and SDS/TX-100 surfactant systems at fairly-low (millimolar) surfactant concentrations. At higher SDS concentrations the microgels were redispersed and ultimately dissolved when mixed with only SDS, but remained precipitated in SDS/TX-100 mixtures. Furthermore, the electrostatic binding of SDS to quaternized chitosan diminished its antibacterial activity and (because the SDS-bearing mixtures with strong biocidal activity were limited to low surfactant concentrations) also resulted in limited hydrophobe solubilization. Conversely, microgels mixed with TX-100 maintained their biocidal activity even when the surfactant was in excess, and exhibited good solubilization properties. This suggests that surfactant-based products that use quaternized chitosan microgels as antibacterial agents should optimally be formulated using nonionic surfactants.

1. Introduction

Chitosan is a cationic polyelectrolyte derived from the naturally abundant biopolymer, chitin (Pillai, Paul, & Sharma, 2009; Rinaudo, 2006). It is composed of cationic D-glucosamine and nonionic *N*-acetyl-D-glucosamine monomer units, and is soluble in acidic aqueous solutions (at pH < 6), where the pH-sensitive primary amine groups on the glucosamine monomer units become charged (Rinaudo, 2006). This switchable amine group enables chitosan to form a variety of gel-like structures through its exposure to alkaline solutions (Babak, Merkovich, Desbrieres, & Rinaudo, 2000; Madihally & Matthew, 1999), or its complexation with oppositely-charged counterions (Bodmeier, Chen, & Paeratakul, 1989; Calvo, Remunan-Lopez, Vila-Jato, & Alonso, 1997b), polymers (Douglas & Tabrizian, 2005; Leong, Mao, Truong-Le, Roy, Walsh, & August, 1998; Smitha, Sridhar, & Khan, 2004) and surfactants (Babak, Merkovich, et al., 2000; Babak, Merkovich, Galbraikh, Shtykova, & Rinaudo, 2000). Due to this versatility, chitosan finds countless applications ranging from drug delivery and tissue engineering (Calvo, Remunan-Lopez, Vila-Jato, & Alonso, 1997a; Janes, Calvo, & Alonso, 2001; Madihally & Matthew, 1999; Muzzarelli, 2009), to textiles (Lim & Hudson, 2003, 2004), to foods, cosmetics and shampoos (Rinaudo, 2006).

In recent years, chitosan and its derivatives have also attracted keen interest as antibacterial agents (Helander, Nurmiaho-Lassila, Ahvenainen, Rhoades, & Roller, 2001; Lim & Hudson, 2004; Shi, Neoh, Kang, & Wang, 2006) for textiles (Lim & Hudson, 2003, 2004), medical implants (Shi et al., 2006), wound dressings (Alipour, Nouri, Mokhtari, & Bahrami, 2009) and dentistry (Ji et al., 2009). Their antibacterial activity is ascribed to the cationic amine groups on their glucosamine monomer units (Helander, Nurmiaho-Lassila, Ahvenainen, Rhoades, & Roller, 2001; Tashiro, 2001), and is further strengthened through the substitution of the glucosamine primary amines with quaternary amines (Lim & Hudson, 2004; Shi et al., 2006). Accordingly, the biocidal activity of "quaternized chitosan" has been demonstrated with a broad range of Gram-positive and

* Corresponding author at: Department of Chemical and Environmental Engineering, University of Toledo, Toledo, OH 43606, United States. Tel.: +1 419 530 8254; fax: +1 419 530 8086.
E-mail address: yakov.lapitsky@utoledo.edu (Y. Lapitsky).

0144-8617/$ – see front matter © 2012 Elsevier Ltd. All rights reserved.
http://dx.doi.org/10.1016/j.carbpol.2012.12.054

Gram-negative bacteria, as well as fungi (Chi, Qin, Zeng, Li, & Wang, 2007; Ji et al., 2009; Lim & Hudson, 2004; Shi et al., 2006; Wang, Du, Yang, Tang, & Luo, 2008). In addition to enhancing the antibacterial activity, the quaternization of chitosan also enhances its solubility at neutral and alkaline pH levels (Cho, Grant, Piquette-Miller, & Allen, 2006; Lim & Hudson, 2004), thereby making it even more versatile. Furthermore, when chitosan or its quaternized derivatives are prepared as crosslinked particles (i.e., micro- or nanogels), their antibacterial activity has been reported to be even greater than that of the chitosan derivatives in their molecular form (Shi et al., 2006).

Building on these findings, here we explore the use of quaternized chitosan microgels for the preparation of antibacterial surfactant mixtures for potential use in cleaning and personal care products. Antibacterial surfactant formulations are often prepared using cationic surfactants (e.g., alkyltrimethylammonium salts). These surfactants, however, are toxic. Consequently, their use in cleaning formulations raises environmental concerns (Garcia, Ribosa, Guindulain, Sanchez-Leal, & Vives-Rego, 2001; Holmberg, Jonsson, Kronberg, & Lindman, 2003; Juergensen, Busnarda, Caux, & Kent, 2000; Li & Brownawell, 2010; Sandbacka, Christianson, & Isomaa, 2000). To this end, dilute chitosan-based microgel dispersions (mixed with less-toxic surfactants) may be attractive substitutes to cationic surfactants and other toxic antibacterial agents (e.g., bleach and triclosan). These microgels are antibacterial even at very low concentrations (Shi et al., 2006) and are cytocompatible with mammalian cells (Lapitsky, Zahir, & Shoichet, 2008; Shi et al., 2006).

Despite these advantages, formulating chitosan-based microgel mixtures with surfactants is not trivial due to the electrostatic binding between oppositely charged surfactants and polymers (Goddard, 1986; Langevin, 2009). This binding can lead to the precipitation of surfactant/polymer complexes (Goddard, 1986; Kastner, Hoffmann, Donges, & Ehrler, 1996; Thalberg, Lindman, & Bergfeldt, 1991; Thalberg, Lindman, & Karlstrom, 1991), thereby complicating the formulation of single-phase surfactant/microgel mixtures (Bradley & Vincent, 2008). Furthermore, by binding to the chitosan, the surfactant may reduce the availability of the cationic amine groups that underlie the biocidal activity of the microgels (which could inactivate their antibacterial properties). To address these challenges and develop guidelines for preparing antibacterial surfactant/microgel formulations, we explored the use of anionic, nonionic and anionic/nonionic surfactant systems. The binding of anionic and nonionic surfactants to the microgels was probed by electrophoretic light scattering and isothermal titration calorimetry (ITC). Once these molecular interactions were characterized, we focused on three key properties of surfactant/chitosan-based microgel mixtures: (1) their colloidal stability, which is essential for maintaining the formulation in a single phase; (2) their antibacterial activity, which is necessary to inactivate bacteria using minimal microgel quantities; and (3) their hydrophobe solubilization properties, which reflect their ability to remove soils or deliver essential oils. Furthermore, we explored the effect of surfactants on dispersion clarity, which is often desirable for designing aesthetically-appealing products.

2. Materials and methods

2.1. Materials

All experiments were performed using Millipore Direct Q-3 deionized water (18.0–18.2 MΩ m resistivity). Chitosan (90% degree of deacetylation, as determined by pH titration), sodium tripolyphosphate (TPP), Triton X-100 (TX-100), glycidyltrimethylammonium chloride and guaiazulene were purchased from Sigma–Aldrich (St. Louis, MO). Ultrapure sodium dodecyl sulfate (SDS) was purchased from MP Biomedicals (Solon, OH), and sodium chloride (NaCl) was purchased from Fisher Scientific (Fair Lawn, NJ, USA). All materials were used as received.

2.2. Synthesis of quaternized chitosan

The antibacterial quaternized chitosan derivative, N-[(2-hydroxy-3-trimethylammonium) propyl] chitosan chloride (HTCC), was prepared through a modified procedure of Lim and Hudson (2004). Briefly, 2.0 g of chitosan flakes were dispersed in 38 mL of water at 85 °C and agitated with a magnetic stirrer. Three 2.45 mL aliquots of glycidyltrimetylammonium chloride were then added to the dispersion at 2 h intervals, and allowed to react for 12 h. The quaternization then became apparent from the dissolution of chitosan flakes, which are otherwise insoluble at neutral and high pH. After the reaction, the HTCC was purified by dialyzing once against 10 mM NaCl and thrice against deionized water (for 12 h each time) through a Spectra/Por regenerated cellulose membrane (molecular weight cutoff = 2000). The final product was then freeze dried for 48 h on a Labconco Freeze Dryer 3 lyophilizer (Kansas City, MO) and characterized by ^{1}H NMR to confirm that the product spectra (not shown) matched the literature spectra for HTCC (Cho et al., 2006). The degree of quaternization was determined to be near-quantitative via conductometric $AgNO_3$ titration, using the procedure of Lim and Hudson (2004).

2.3. Microgel preparation

The quaternized chitosan microgels were prepared through the ionic crosslinking of HTCC with the pentavalent anion, TPP, as done in previous studies (Shi et al., 2006; Zhang, Mardyani, Chan, & Kumacheva, 2006). Briefly, 3.3 mL of 0.1 wt% TPP solution were added dropwise (at a rate of 200 μL/min) to 15 mL of 0.1 wt% HTCC solution, where each solution contained 10 mM NaCl. The addition rate was controlled with a Fisher Scientific syringe pump (Model # 78-0100I), and the receiving HTCC solution was stirred with a cylindrical (12 mm × 4 mm) magnetic stir bar at 800 RPM inside a 20 mL scintillation vial. The microgels were then allowed to equilibrate for 15 min, whereupon their size distributions and ζ-potentials were characterized by dynamic and electrophoretic light scattering.

2.4. Isothermal titration calorimetry

The binding of SDS and TX-100 to the microgels was tested by isothermal titration calorimetry (ITC), using a Microcal VP-ITC instrument (GE Healthcare, Northampton, MA). In each measurement, twenty five 10-μL injections of 40 mmol/kg surfactant (either SDS or TX-100) solution (containing 10 mM NaCl) were added to a 1.48 mL sample cell filled with microgel dispersions (described in Section 2.3) at a matching NaCl concentration. To account for the heat of surfactant dilution (and demicellization), control measurements were also performed, where 40 mM surfactant solutions were injected into microgel-free 10 mM NaCl solutions. The enthalpic signal due to binding was then obtained (as the heat absorbed from the sample cell per mole of added surfactant) by subtracting this heat of dilution from the signal obtained from the addition of surfactant to the microgels (Lapitsky, Parikh, & Kaler, 2007; Matulis, Rouzina, & Bloomfield, 2002).

2.5. Dynamic and electrophoretic light scattering

To determine the effect of surfactant on the size distribution and surface charge of the chitosan-based microgels, the dispersions were probed by dynamic and electrophoretic light scattering. These measurements were performed using a Zetasizer Nano ZS instrument (Malvern, Worcestershire, UK). The

effect of surfactant binding on the microgel surface charge was inferred from the changes in ζ-potential, which were estimated from the electrophoretic light scattering measurements using the Helmholtz–Smoluchowski equation (Hiemenz & Rajagoplan, 1997). The effects of the SDS and SDS/TX-100 surfactant systems on microgel size (which reflected the microgel aggregation states) were measured by dynamic light scattering (DLS), based on changes in the *z*-average hydrodynamic diameters (estimated by the cumulant analysis (Hiemenz & Rajagoplan, 1997)). Conversely, the effects of TX-100 on microgel aggregation, were characterized by analyzing the DLS data by the multiple narrow modes algorithm (Nobbmann & Morfesis, 2008). This was because the microgels remained dispersed in a single phase even at high surfactant concentrations (where the scattering from the micelles became significant), and the multiple narrow modes algorithm allowed the scattering signal from the microgels to be resolved from that of the TX-100 micelles.

2.6. Colloidal stability of surfactant/microgel mixtures

The short-term colloidal stability of surfactant/microgel mixtures was characterized through visual observation and DLS, by adapting the titration procedure of Wang, Kimura, Huang, Dubin, and Jaeger (1999) and Wang, Kimura, Dubin, and Jaeger (2000). Here, concentrated surfactant solutions (containing either 10 mmol/kg SDS, 14.3 mmol/kg 70:30 SDS:TX-100, 25 mmol/kg 40:60 SDS:TX-100, 100 mmol/kg 10:90 SDS:TX-100, or 100 mmol/kg TX-100) were titrated into the microgel dispersions described in Section 2.3 in 65–250-μL increments. During the titrations the surfactant/microgel mixtures were continuously stirred at 800 rpm using a cylindrical (12 mm × 4 mm) magnetic stir bar, and equilibrated for 6 min after each surfactant addition prior to visual analysis and DLS characterization. Each titration was performed three times and yielded reproducible results. The long-term colloidal stability was then tested by equilibrating the samples at room temperature over 6 weeks and monitoring them for precipitation.

2.7. Antibacterial activity tests

The effect of anionic and nonionic surfactants on the microgel antibacterial properties was probed using *Pseudomonas aeruginosa* (*P. aeruginosa*; wild-type PAO1 strain) as a model Gram-negative bacterium. This bacterium was selected due to its strong resistance to quaternized chitosan, which to our knowledge was the highest of all bacteria tested to date (Chi et al., 2007; Wang et al., 2008). The bacteria were cultured in one-tenth strength LB broth (2.5 g/L, Difco Laboratory, Detroit, MI) at 37 °C until the late-exponential phase. The cells were then harvested by centrifugation at 2000 × *g* for 15 min using an Eppendorf 5804R centrifuge (Hamburg, Germany), washed and resuspended in phosphate buffer (0.54 g Na_2HPO_4 and 0.88 g KH_2PO_4/L, pH 6.98) (Thurston-Enriquez, Haas, Jacangelo, & Gerba, 2003) as bacterial suspensions ($OD_{600} = 0.25 \pm 0.02$).

All glassware used in this experiment was sterilized in an autoclave. Likewise, the HTCC, TPP and surfactant solutions used to prepare the surfactant/microgel dispersions were sterile-filtered using Santorius Minisart NML 0.8 μm syringe filters. After the filtration, the microgels were prepared inside a BSL 2 certified biosafety chamber (using the procedure in Section 2.3), whereupon 2 mL of surfactant solution (which contained either SDS, TX-100 or a mixture of both) were added at a rate of 1 mL/min, such that the final HTCC concentration was 7.4×10^{-2} wt%. Each antimicrobial dispersion was then tested in triplicate at room temperature (22 ± 2 °C). The bacterial suspension was mixed with the surfactant/microgel dispersions in a 1:100 ratio (150 μL:15 mL). After mixing, samples were taken at 5, 15, and 30 min to quantify the effect of surfactant/microgel mixtures on the number of viable cells. The viable cells were enumerated at each time point using the heterotrophic plate count method with R2A agar plates (Difco Laboratories, Detroit, MI).

2.8. Dye solubilization tests

To test the hydrophobe solubilization properties of each surfactant/microgel mixture type, surfactant/microgel dispersions were prepared as described previously using SDS:TX-100 ratios of 100:0, 70:30, 40:60, 10:90 and 0:100, and total surfactant concentrations of 1.75, 1.12, 1.04, 1.08 and 14.4 mmol/kg, respectively. The concentrations of SDS-containing samples corresponded to the maximum surfactant concentrations that were mixed with the microgels before rapid precipitation occurred (see Section 3.2.1). Conversely, the concentration of 14.4 mmol/kg was used for the 0:100 SDS:TX-100 system (in which rapid precipitation did not occur) because it was the highest surfactant concentration tested in the colloidal stability and biocidal activity experiments. Three milliliters of each dispersion type were added to a test tube and mixed with 0.2 g of hydrophobic guaiazulene dye for 5 min on a vortex mixer. The samples were then equilibrated for 24 h and – after removing the microgels and undissolved dye particles by passing the dispersions through a Millipore Millex® FG 0.2 μm filter (to minimize artifacts due to light scattering and absorption from the microgels and undissolved dye) – quantified for the dissolved dye content by UV/vis spectroscopy ($\lambda = 603$ nm; extinction coefficient = 0.2575 $mM^{-1}\ cm^{-1}$) using a Cary 50 spectrophotometer (Varian Inc., Palo Alto, CA). Each measurement was performed in triplicate.

2.9. Turbidimetric measurements

To probe the effect of surfactant choice on formulation clarity, the turbidity of each dispersion used in the dye solubilization experiment was quantified. This choice of dispersion compositions reflected two considerations: (1) these surfactant concentrations optimize hydrophobe solubilization without diminishing biocidal activity; and (2) because the turbidity increases with the surfactant content, these compositions enable the measurement of maximum turbidity in the stable surfactant/microgel dispersions obtained using each surfactant system. Here, the turbidity of dye-free surfactant/microgel dispersions was measured (without filtration at $\lambda = 488$ nm) immediately after surfactant addition, using a Cary 50 spectrophotometer. Each measurement was performed thrice.

3. Results and discussion

3.1. Surfactant binding to chitosan-derived microgels

The binding of anionic SDS and nonionic TX-100 to the microgels was probed by ITC and electrophoretic light scattering. When SDS was titrated into the microgel dispersion, an exothermic binding heat (of approximately 5 kJ/mol of added SDS) was detected by ITC (Fig. 1), thus indicating that the SDS was binding to the microgels. Once the SDS concentration exceeded ~2 mmol/kg, however, the binding heat diminished sharply to ~0.7–0.8 kJ/mol. This transition suggests the saturation of cationic binding sites (Lapitsky et al., 2007; Matulis et al., 2002). The persistence of the exothermic binding heat beyond that point, however, suggests that SDS continues to bind even after the cationic charges are saturated. Conversely, no binding heat was detected when TX-100 was added to the microgels, thus suggesting that TX-100 does not bind to the chitosan-derived microgels.

This interpretation of the molecular binding events is further supported by the ζ-potential estimates obtained by electrophoretic light scattering. Without surfactant, the microgel ζ-potential in

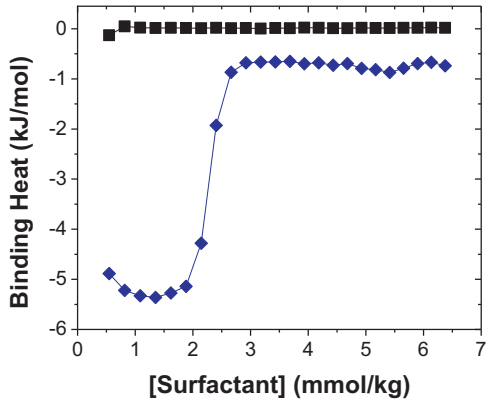

Fig. 1. ITC data for (♦) SDS and (■) TX-100 binding to chitosan-based microgels. The lines are guides to the eye.

10 mM NaCl is ~15 mV (see Fig. 2). When SDS is added to the microgels, the ζ-potential stays nearly constant, until the SDS concentration reaches the saturation transition in the ITC data (i.e., exceeded ~2 mmol/kg). At this point, the ζ-potential diminishes dramatically and ultimately becomes negative. The microgel charge inversion that occurs after the saturation of cationic sites confirms the continued binding of SDS to the microgels, which likely occurs through hydrophobic association (Ohbu, Hiraishi, & Kashiwa, 1982). Not surprisingly, the addition of nonionic TX-100 (instead of the SDS) has no effect on the microgel ζ-potential. This combination of ITC and electrophoretic light scattering data suggests that SDS binds to the chitosan-derived microgels and the TX-100 does not.

3.2. Colloidal stability of surfactant/microgel mixtures

3.2.1. Short-term colloidal stability

To determine the surfactant compositions at which the microgels can be dispersed, the short-term colloidal stability of the surfactant/microgel mixtures was investigated by titrating concentrated surfactant solutions into dilute microgel dispersions (which initially contained 8.2×10^{-2} wt% HTCC). Microgel aggregation was then tracked both visually and by DLS, allowing the mixtures to equilibrate for 6 min after each surfactant addition. When SDS was used, the microgels – whose *z*-average hydrodynamic diameter was ca. 300 nm – remained dispersed until the surfactant was mixed with the cationic microgels near the saturation point ([SDS] ~ 2 mmol/kg, as shown by the ITC data in Section 3.1 and the blue diamonds in Fig. 3a). Above this point, their z-average

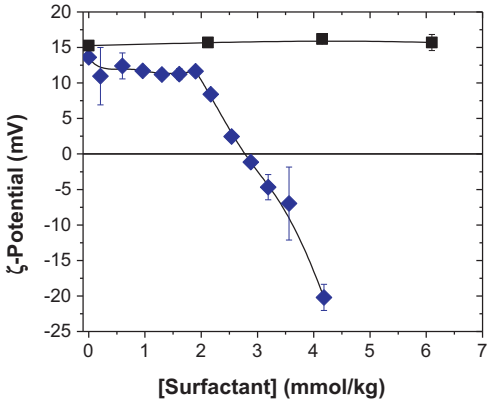

Fig. 2. Microgel ζ-potentials in the presence of (♦) SDS and (■) TX-100. The lines are guides to the eye.

Table 1
Concentrations of SDS and total surfactant at the onset of rapid precipitation.

SDS:TX-100 molar ratio	[SDS] at precipitation point (mmol/kg)	[SDS] + [TX-100] at precipitation point (mmol/kg)
100:0	1.89 ± 0.14	1.89 ± 0.14
70:30	0.95 ± 0.17	1.37 ± 0.25
40:60	0.60 ± 0.18	1.50 ± 0.46
10:90	0.16 ± 0.05	1.60 ± 0.52

diameters (Fig. 3) and polydispersities (Supplementary Data, Fig. S1) increased sharply due to coagulation, and the microgels precipitated. This coagulation likely reflects the neutralization of the HTCC charges on the microgel surface (Bradley & Vincent, 2008; Goddard, 1986; Lapitsky et al., 2007), which diminishes both the hydrophilicity of the microgels and the electrostatic stabilization of their dispersions.

When the SDS concentration was raised further, above 8 mmol/kg, the precipitate was resolubilized (data not shown). These transitions are consistent with previous studies on the interactions of molecular HTCC (Lapitsky et al., 2008) and cationically-modified hydroxyethyl cellulose (Goddard, 1986; Kastner et al., 1996) with anionic surfactants – i.e., where the surfactant/polyelectrolyte complexes precipitated when the surfactant and polymer were mixed at near stoichiometric ratios, and were resolubilized in the limit of high surfactant concentration (Goddard, 1986; Kastner et al., 1996; Lapitsky et al., 2008). This redissolution phenomenon is attributed to the additional binding of surfactant, which breaks up the interpolymer surfactant/polyelectrolyte aggregates, such that the polymer-bound surfactant aggregates are no longer shared by multiple polymer chains (Goddard, 1986).

Interestingly, the microgel hydrodynamic diameter diminished dramatically as the concentration was increased beyond the resolubilization boundary (data not shown), and matched that obtained for SDS complexes with molecular (TPP-free) HTCC. This decrease in particle size was accompanied by a sharp reduction in dispersion turbidity, thus indicating microgel dissolution and suggesting that the binding of SDS can displace ionic crosslinks formed by TPP between the HTCC chains. This view was further supported by comparing the ITC data for SDS binding to HTCC/TPP microgels – where most of the binding sites were initially occupied by TPP – with its binding to molecular HTCC (without TPP), where all the binding sites were initially free. This comparison (see Supplementary Data, Fig. S2) revealed that the presence of TPP had little impact on the SDS concentration required to saturate the cationic HTCC binding sites. Thus, the electrostatic binding of SDS can displace the TPP crosslinks within the microgels, and can lead to their dissolution when SDS is in excess.

When the surfactant titrations were repeated using tertiary SDS/TX-100/water mixtures (where the SDS:TX-100 ratios were either 70:30, 40:60 or 10:90), the addition of TX-100 shifted the rapid precipitation boundary to lower SDS concentrations (see Fig. 3a and Table 1). Indeed, at each SDS:TX-100 ratio rapid precipitation occurred at roughly the same overall surfactant concentration (roughly 1.4–2 mmol/kg, as shown in Fig. 3b and Table 1). This shift of the precipitation boundary to lower SDS concentrations did not occur when molecular HTCC was used instead of the microgels (data not shown), and was particularly surprising because the microgel ζ-potential in SDS/TX-100/water surfactant mixtures was roughly the same as that in the absence of TX-100 at the same SDS concentration (Supplementary Data, Fig. S3). Furthermore, unlike in the SDS/microgel mixtures without TX-100, the microgels did not redisperse (or dissolve) in SDS/TX-100 surfactant mixtures at higher concentrations (up to 100 mmol/kg).

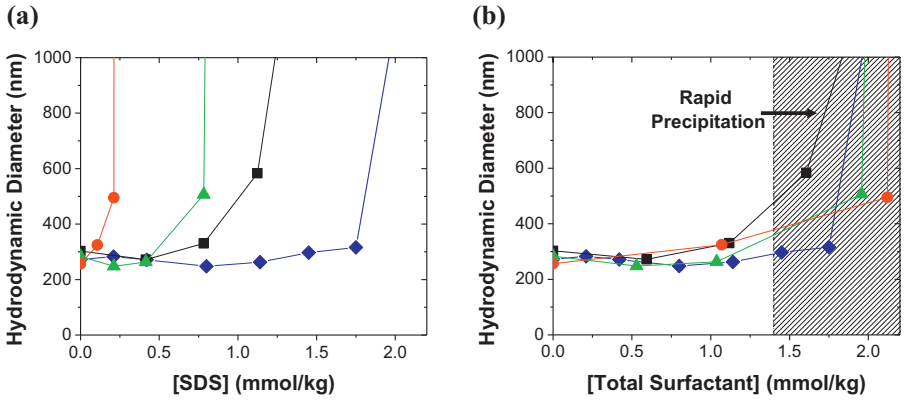

Fig. 3. Dynamic light scattering analysis of cationic microgel dispersions in SDS/TX-100 solutions with (♦) 100:0, (■) 70:30, (▲) 40:60 and (●) 10:90 SDS:TX-100 molar ratios, shown as function of (a) SDS concentration and (b) total surfactant concentration (with the onset of rapid precipitation highlighted by the shaded region). The solid lines are guides to the eye.

The titration experiment was also repeated using nonionic TX-100 as the only surfactant species, thereby eliminating electrostatic surfactant/microgel binding. Not surprisingly, the microgels remained dispersed at all investigated surfactant concentrations ([TX-100] ≤ 14.4 mmol/kg) and, as shown by the DLS data in Fig. 4 – where the growing peak at 8 nm reflects the formation of TX-100 micelles (Streletzky & Phillies, 1995) – the addition of surfactant had little impact on the microgel size distributions. This suggests that surfactant-induced coagulation of cationic microgel dispersions can best be avoided using nonionic surfactant systems.

3.2.2. Long-term colloidal stability

The short-term colloidal stability data in Section 3.2.1 reveals the restrictions on the surfactant compositions that can be used with the HTCC/TPP microgels. In addition to the rapid, surfactant-induced microgel coagulation (or disintegration), however, the long-term stability of these colloidal dispersions (which is essential for their commercial use) can be undermined by other effects – e.g., attractive Van der Waals interactions (Rasmusson, Routh, & Vincent, 2004; Wu, Huang, & Hu, 2003), bridging flocculation by surface-bound TPP (Huang & Lapitsky, 2011) or hydrolytic degradation (Morris, Castile, Smith, Adams, & Harding, 2011). To address this, we investigated the stability of these dispersions over longer timescales.

Upon storage at room temperature, the microgels eventually coagulated and precipitated at all investigated surfactant concentrations (and even without added surfactant). At low surfactant concentrations (0–2 mmol/kg), below the onset of rapid precipitation in microgel mixtures with SDS and SDS/TX-100 (see Fig. 3 and Table 1), precipitation occurred within one or two days. This limited colloidal stability of HTCC/TPP microgels differs greatly from that of non-quaternized chitosan/TPP microgels, which remain dispersed even after several months (Morris, Castile, Smith, Adams, & Harding, 2011; Tsai, Chen, Bai, & Chen, 2011). This may reflect differences in the biopolymer/TPP binding strength, which ITC measurements suggest to be significantly weaker for HTCC than for chitosan (see Supplementary Data, Fig. S4). A recent study on the coagulation of chitosan/TPP microgels has suggested microgel coagulation to occur through the ionic bridging of the microgels by TPP, which occurs more rapidly at higher free TPP concentrations (Huang & Lapitsky, 2011). The free TPP concentration, on the other hand, scales inversely with the binding strength; thus, the faster coagulation of HTCC/TPP microgels might reflect the higher concentration of bridging TPP ions remaining in solution. This "TPP bridging" coagulation mechanism is also supported by more-recent preliminary experiments (data not shown) where the shelf life of the surfactant-free microgel dispersion was extended more than tenfold by tuning the TPP concentration used to prepare the microgels.

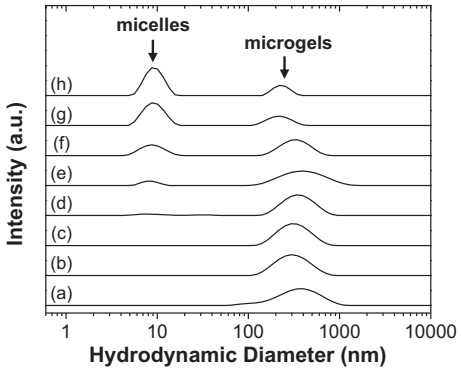

Fig. 4. DLS analysis of microgel size distributions in (a) 0 mmol/kg, (b) 2.1 mmol/kg, (c) 4.2 mmol/kg, (d) 6.1 mmol/kg, (e) 8.0 mmol/kg, (f) 9.8 mmol/kg, (g) 11.5 mmol/kg, and (h) 14.4 mmol/kg TX-100 solutions. The curves were offset vertically for clarity.

When surfactant/microgel mixtures were prepared at higher (nonionic) surfactant concentrations, the colloidal stability was dramatically improved. For example, when the microgels were mixed with 14.4 mmol/kg TX-100, they remained dispersed for 5–6 weeks. This extended shelf life suggests that, in addition to not causing precipitation, TX-100 dramatically enhances the long-term colloidal stability of HTCC microgel dispersions. It also indicates that, despite the lack of binding signal in the ITC data (see Fig. 1), the nonionic TX-100 might interact hydrophobically with HTCC/TPP microgels (which is consistent with the interactions reported for chitosan mixtures with TX-100 (Chatterjee, Chatterjee, & Woo, 2010) and other nonionic surfactants (Grant, Lee, Liu, & Allen, 2008; Pepic, Filipovic-Grcic, & Jalsenjak, 2008).

3.3. Antibacterial activity of surfactant/microgel mixtures

The antibacterial activity of the surfactant/microgel dispersions was tested using *P. aeruginosa* PAO1 (an opportunistic human pathogen) as a model Gram-negative bacterium. As a positive control, the bacteria were added to a surfactant-free microgel dispersion (containing 7.4×10^{-2} wt% HTCC), whereupon all bacteria were rapidly killed within the first 5 min of the experiment (Fig. 5, Group 1; where the number of viable cells, N, is normalized by their initial number, N_0). When SDS was added to the dispersion, such that the microgel cationic charges were not fully neutralized (i.e.,

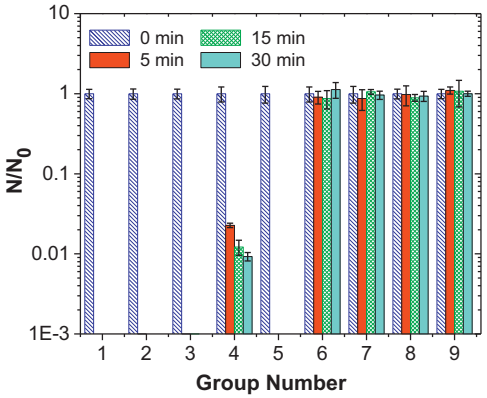

Fig. 5. Normalized *P. aeruginosa* viable cell counts after 0–30 min of exposure to microgels mixed with (1) water, (2) 1.0 mmol/kg SDS, (3) 3.0 mmol/kg 40:60 SDS/TX-100 mixture, (4) 10 mmol/kg SDS and (5) 14.4 mmol/kg TX-100, and microgels-free solutions containing (6) 10 mmol/kg SDS, (7) 14.4 mmol/kg TX-100, (8) 3.0 mmol/kg 40:60 SDS/TX-100 mixture, and (9) water.

1 mmol/kg SDS; see Group 2), the microgels maintained their strong antibacterial activity and again killed all the bacteria within 5 min. Similar results were obtained when the microgels were dispersed in a dilute (3 mmol/kg; see Fig. 5, Group 3) 40:60 SDS:TX-100 mixture, which had a similar SDS concentration to Group 2. Interestingly, the coagulation of the microgels at this SDS/TX-100 surfactant concentration (see Fig. 3) did not appear to affect their antibacterial properties. When the SDS concentration was raised to be in excess to the HTCC amines, however (where the microgels dissolve; using 10 mmol/kg SDS), the antibacterial activity diminished, with nearly 1% of the bacteria still viable after 30 min of contact time (Fig. 5, Group 4). This reduction in antibacterial activity likely reflects the neutralization of the quaternary HTCC amine groups (to which the antibacterial activity is typically attributed (Helander et al., 2001; Tashiro, 2001) by the microgel-bound anionic surfactant. The neutralization is evident from the ζ-potential data in Fig. 2, where the microgel charge became negative at SDS concentrations above 2.8 mmol/kg. Furthermore, because the antibacterial activity of microgels may be stronger than that of molecular HTCC (Shi et al., 2006), the reduced antibacterial activity at higher SDS concentrations might also reflect microgel dissociation. Thus, the electrostatic binding of anionic surfactant to the cationic microgels can reduce both the stability and antibacterial activity of the mixture. Conversely, when an excess (14.4 mmol/kg) of the non-binding TX-100 was added to the microgels, the strong antibacterial properties were preserved (Fig. 5, Group 5), and all of the bacteria were killed within 5 min of contact time. This suggests that, by avoiding electrostatic binding, antibacterial activity of chitosan-based microgels can be preserved even at high surfactant concentrations.

To ensure that the surfactants used in this study were not biocidal on their own, the cells were exposed to microgel-free SDS, TX-100 and SDS/TX-100 surfactant solutions (Groups 6–8) and water (Group 9) as negative controls. These measurements confirmed that, without the microgels, the surfactants (Groups 6–8) had no short-term effect on bacterial viability, and that the rapid antibacterial activity of the surfactant/microgel mixtures stemmed from the quaternized chitosan and not the surfactants. Likewise, when the bacteria were exposed to water (without surfactant or microgels; Group 9), the viable cell counts remained constant over the 30 min experiment. Consistent with the previous work on antibacterial polycations (Murata, Koepsel, Matyjaszewski, & Russell, 2007; Tashiro, 2001), these findings suggest that the strong antibacterial properties of chitosan-based microgels are mediated by their cationic amine groups. Accordingly, in formulations containing nonionic and anionic surfactants, best antibacterial activity is achieved using either nonionic surfactants, or anionic surfactants at low concentrations (where the microgel amine groups are not neutralized).

The high antibacterial activity of non-neutralized HTCC microgels is also consistent with previous studies on the biocidal properties of HTCC against various Gram-positive and Gram-negative bacteria (Chi et al., 2007; Ji et al., 2009; Lim & Hudson, 2004; Shi et al., 2006; Wang et al., 2008). Although the antibacterial activity test on the surfactant/HTCC microgel mixtures was performed with only one bacterial strain, the model bacterium used in this experiment (*P. aeruginosa*) has shown the strongest resistance to HTCC reported to date (Chi et al., 2007; Wang et al., 2008). Thus, the antibacterial activity of HTCC microgels against *P. aeruginosa* suggests that, as long as the microgel amine groups are not neutralized, the microgels should retain their strong antibacterial properties against other bacterial strains. This result (combined with the previous studies on the biocidal properties of HTCC with a wide range of bacteria) suggests that HTCC microgels could indeed be an attractive replacement to cationic surfactants and other toxic antibacterial agents (e.g., triclosan or bleach).

3.4. Hydrophobe solubilization properties of surfactant/microgel mixtures

In addition to their colloidal stability and antibacterial properties, successful cleaning and personal care product formulations should solubilize hydrophobic compounds. Thus, hydrophobe solubilization properties of surfactant/microgel mixtures were measured. The surfactant concentrations in dispersions prepared using the SDS and SDS/TX-100 surfactant systems were selected to be near the onset of rapid precipitation (as described in Section 2.8; see Fig. 3b), such that the surfactant content was near the maximum that can be used without undermining the stability or antibacterial activity of the dispersion. Similarly, dispersions prepared using only TX-100 – where no rapid precipitation or antibacterial activity reduction occurred – were prepared at the maximum TX-100 concentration used in the colloidal stability and antibacterial activity tests (i.e., 14.4 mmol/kg TX-100).

To test the hydrophobe solubilization properties of the surfactant/microgel mixtures, the dispersions were mixed with hydrophobic blue (guaiazulene) dye. When the dye was mixed with the surfactant/microgel dispersions, a fraction of the dye dissolved in samples containing TX-100 or SDS/TX-100 mixtures. This was evident from the blue color of the surfactant/microgel dispersion (see Fig. 6a, Samples ii–v), and confirmed by UV–vis spectroscopy (Fig. 6b). No dye dissolution, however, occurred in dispersions containing SDS without TX-100 (Fig. 6a, Sample i and b).

Interestingly, microgel dispersions prepared using 70:30 and 40:60 SDS:TX-100 ratios also generated finely-dispersed dye particles, which were not solubilized at the molecular level. Most of these particles (along with the microgels) were removed by filtration through a 0.2 μm filter prior to spectroscopic analysis. The dye particles at the 40:60 SDS:TX-100 ratio, however, were dispersed more-finely than those at 70:30 SDS:TX-100. Consequently, the filtration of 70:30 SDS:TX-100 samples yielded clear solutions, while the filtered 40:60 SDS:TX-100 samples remained opaque. This indicated that nearly all undissolved particles were removed from the 70:30 SDS:TX-100 sample, while in the 40:60 SDS:TX-100 samples some of the dye particles remained dispersed. The presence of finely-dispersed dye particles in the 40:60 SDS:TX-100 samples made the measured solubilized dye concentration (in Fig. 6b) appear higher than it really was (and higher than it was in other

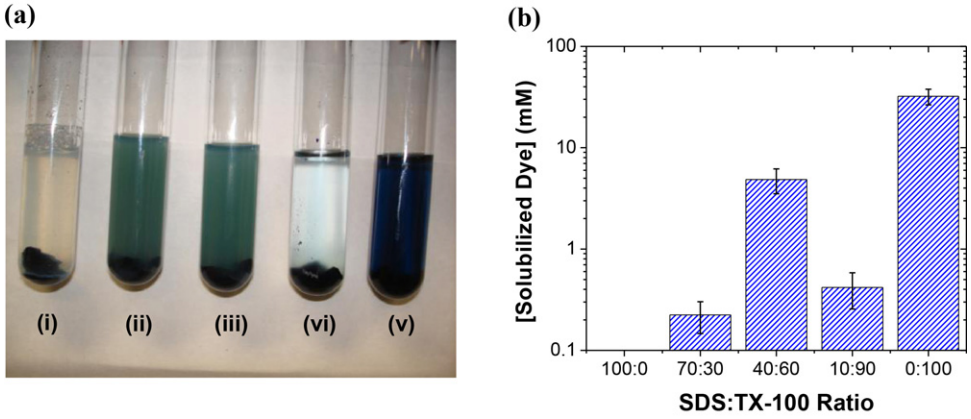

Fig. 6. Visual observation (a) and spectroscopic quantification (b) of guaiazulene dye solubilization in surfactant/microgel dispersions containing (i) 1.75 mmol/kg SDS, (ii) 1.12 mmol/kg 70:30 SDS:TX-100, (iii) 1.04 mmol/kg 40:60 SDS:TX-100, (iv) 1.09 mmol/kg 10:90 SDS:TX-100, and (v) 14.4 mmol/kg TX-100. The spectroscopic analysis was performed after filtering out the microgels and larger dispersed dye particles from the samples.

SDS-bearing samples). Because of this artifact, the true dye solubility in the 40:60 SDS:TX-100/microgel mixture was lower than it appeared in the UV–vis measurements. The microgels dispersed in 14.4 mmol/kg TX-100, however, had by far the best solubilization properties (where the solubilized dye concentration was almost seven times higher than that measured for the 40:60 SDS:TX-100 samples).

The lack of dissolved dye in dispersions containing only SDS likely reflected the fact that almost all of the SDS was taken up by the microgels, and was therefore unavailable to interact with the dye. The impact of SDS uptake on dye solubilization was confirmed by mixing the dye with microgel-free 1.75 mmol/kg SDS (i.e., the SDS concentration in Fig. 6, Sample i), which yielded a dark blue mixture with finely-dispersed dye particles (see Supplementary Data, Fig. S5). Conversely, when SDS/TX-100 mixtures were used, a substantial portion of the surfactant remained outside the microgels, and enabled dye solubilization. The stable dye particle dispersions that form at higher, (70:30 and 40:60) SDS:TX-100 ratios may result from the electrostatic repulsion that exists between dye particles coated with anionic surfactant, and suggest that the surfactant/microgel mixtures may be able to remove hydrophobic soils without molecular solubilization. However, because the SDS-free microgel/TX-100 formulation can be prepared at higher surfactant concentrations (without inducing rapid precipitation or compromising antibacterial activity), the nonionic surfactant-based mixtures provide the best solubilization properties.

3.5. Effects of surfactant on mixture turbidity

Besides being functional, consumer product formulations should be aesthetically-appealing. For products sold in clear packaging, clarity is a key optical property. To this end, we have characterized the effect of surfactant on the turbidity of the chitosan-based microgel dispersions at the same surfactant concentrations as were used in the hydrophobe solubilization tests (see Fig. 7). The dispersion clarity depended strongly on the SDS content. When only SDS was added to the microgels (without TX-100), the turbidity increased dramatically, despite the nearly-constant hydrodynamic diameter of the microgels (see Fig. 3). This reflects a greater refractive index contrast between the microgel and solvent phases, which stems from the uptake of organic SDS molecules into the aqueous microgel particles. When SDS/TX-100 surfactant mixtures were used, the turbidity increase became progressively less-pronounced with decreasing SDS:TX-100 ratios, suggesting a smaller extent of surfactant uptake by the microgels. Likewise, when SDS-free TX-100 was used, the turbidity remained virtually unchanged by the addition of surfactant. This suggests that the clarity of the nonionic surfactant/microgel dispersions is not diminished by the uptake of surfactants into the microgels (like it is in the case of anionic surfactants), and that microgel mixtures with nonionic surfactants exhibit superior optical properties to their anionic surfactant-containing counterparts.

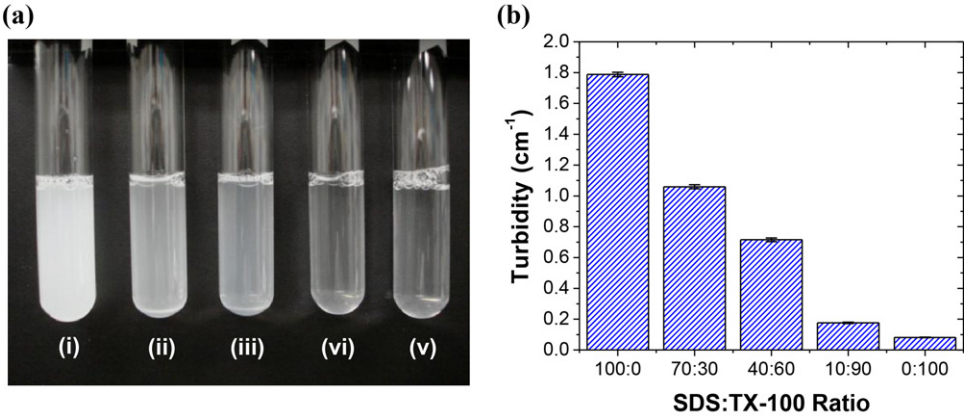

Fig. 7. Visual observation (a) and turbidimetric quantification (b) of how the addition of surfactant at (i) 100:0, (ii) 70:30, (iii) 40:60, (iv) 10:90 and (v) 0:100 SDS:TX-100 ratios affects the dispersion clarity.

4. Conclusions

Chitosan-derived microgels are highly antibacterial, and may be attractive alternatives to cationic surfactants and other toxic antibacterial agents (e.g., bleach and triclosan). We have prepared and characterized their mixtures with model nonionic and anionic surfactants (and with anionic/nonionic surfactant mixtures). This revealed that the mixing of chitosan-derived microgels with a nonionic surfactant (TX-100) preserves their antibacterial activity and low optical density, does not lead to rapid, surfactant-induced precipitation (which limits the range of surfactant concentrations that can be used), and enhances their long-term colloidal stability. Furthermore, because the addition of nonionic surfactant does not undermine the biocidal activity and colloidal stability of the microgels, nonionic surfactant/microgel mixtures can be prepared at high surfactant concentrations, which provide superior hydrophobe solubilization.

Conversely, chitosan-based microgel mixtures with anionic (SDS) and anionic/nonionic (SDS/TX-100) surfactant mixtures undergo rapid, surfactant-induced precipitation. In the case of mixed anionic/nonionic surfactant systems, this limits the mixture compositions to very low surfactant concentrations, which lead to poor hydrophobe solubilization properties. When microgels are mixed with only anionic surfactant, however, the mixtures remain dispersed both in the limits of low and high surfactant concentrations (with surfactant-induced precipitation occurring at intermediate concentrations). Like in the case of the anionic/nonionic surfactant mixtures, mixtures at low anionic surfactant concentration exhibit poor hydrophobe solubilization properties (which are worse than those in anionic/nonionic surfactant mixtures). Conversely, at higher anionic surfactant concentrations (above the CMC), the binding of surfactant to the quaternized chitosan weakens its biocidal activity and ultimately leads to microgel dissolution. Furthermore, the uptake of anionic surfactant by the microgels makes the dispersions more opaque, thereby potentially making the anionic surfactant/microgel mixtures less-suitable for clear packaging. These observations suggest that, to create stable formulations that combine antibacterial activity with good solubilization and optical properties, surfactant/chitosan-based microgel mixtures are best prepared using nonionic surfactant systems.

Acknowledgments

The authors gratefully acknowledge the University of Toledo's College of Engineering and the National Science Foundation (CBET-1133795 and CBET-0933288) for funding and Mr. Steven Westenkirchner for technical assistance with the preliminary work.

Appendix A. Supplementary data

Supplementary data associated with this article can be found, in the online version, at http://dx.doi.org/10.1016/j.carbpol.2012.12.054.

References

Alipour, S. M., Nouri, M., Mokhtari, J., & Bahrami, S. H. (2009). Electrospinning of poly(vinyl alcohol)-water-soluble quaternized chitosan derivative blend. *Carbohydrate Research*, *344*, 2496–2501.

Babak, V. G., Merkovich, E. A., Desbrieres, J., & Rinaudo, M. (2000). Formation of an ordered nanostructure in surfactantpolyelectrolyte complexes formed by interfacial diffusion. *Polymer Bulletin*, *45*, 77–81.

Babak, V. G., Merkovich, E. A., Galbraikh, L. S., Shtykova, E. V., & Rinaudo, M. (2000). Kinetics of diffusionally induced gelation and ordered nanostructure formation in surfactant-polyelectrolyte complexes formed at water/water emulsion type interfaces. *Mendeleev Communications*, *3*, 94.

Bodmeier, R., Chen, H., & Paeratakul, O. (1989). A novel approach to the oral delivery of micro- or nanoparticles. *Pharmaceutical Research*, *6*, 413–417.

Bradley, M., & Vincent, B. (2008). Poly(vinylpyridine) core/poly(N-isopropylacrylamide) shell microgel particles: Their characterization and the uptake and release of an anionic surfactant. *Langmuir*, *24*, 2421–2425.

Calvo, P., Remunan-Lopez, C., Vila-Jato, J. L., & Alonso, M. J. (1997a). Chitosan and chitosan/ethylene oxide-propylene oxide block copolymer nanoparticles as novel carriers for proteins and vaccines. *Pharmaceutical Research*, *14*, 1431–1436.

Calvo, P., Remunan-Lopez, C., Vila-Jato, J. L., & Alonso, M. J. (1997b). Novel hydrophilic chitosan-polyethylene oxide nanoparticles as protein carriers. *Journal of Applied Polymer Science*, *63*, 125–132.

Chatterjee, S., Chatterjee, T., & Woo, S. H. (2010). Enhanced solubilization of phenanthrene in Triton X-100 solutions by the addition of small amounts of chitosan. *Chemical Engineering Journal*, *163*, 450–453.

Chi, W. L., Qin, C. Q., Zeng, L. T., Li, W., & Wang, W. (2007). Microbiocidal activity of chitosan-N-2-hydroxypropyl trimethyl ammonium chloride. *Journal of Applied Polymer Science*, *103*, 3851–3856.

Cho, J., Grant, J., Piquette-Miller, M., & Allen, C. (2006). Synthesis and physicochemical and dynamic mechanical properties of a water-soluble chitosan derivative as a biomaterial. *Biomacromolecules*, *7*, 2845–2855.

Douglas, K. L., & Tabrizian, M. (2005). Effect of experimental parameters on the formation of alginate-chitosan nanoparticles and evaluation of their potential application as DNA carrier. *Journal of Biomaterials Science Polymer Edition*, *16*, 43–56.

Garcia, M. T., Ribosa, I., Guindulain, T., Sanchez-Leal, J., & Vives-Rego, J. (2001). Fate and effect of monoalkyl quaternary ammonium surfactants in the aquatic environment. *Environmental Pollution*, *111*, 169–175.

Goddard, E. D. (1986). Polymer surfactant interaction. 2. Polymer and surfactant of opposite charge. *Colloids and Surfaces*, *19*, 301–329.

Grant, J., Lee, H., Liu, R. C. W., & Allen, C. (2008). Intermolecular interactions and morphology of aqeous polymer/surfactant mixtures containing cationic chitosan and nonionic sorbitan esters. *Biomacromolecules*, *9*, 2146–2152.

Helander, I. M., Nurmiaho-Lassila, E. L., Ahvenainen, R., Rhoades, J., & Roller, S. (2001). Chitosan disrupts the barrier properties of the outer membrane of Gram-negative bacteria. *International Journal of Food Microbiology*, *71*, 235–244.

Hiemenz, P. C., & Rajagoplan, R. (1997). *Principles of colloid and surface chemistry*. New York: Marcel Dekker, Inc.

Holmberg, K., Jonsson, B., Kronberg, B., & Lindman, B. (2003). *Surfactants and polymers in aqueous solutions*. New York: John Wiley & Sons.

Huang, Y., & Lapitsky, Y. (2011). Monovalent salt enhances colloidal stability during the formation of chitosan/tripolyphosphate microgels. *Langmuir*, *27*, 10392–10399.

Janes, K. A., Calvo, P., & Alonso, M. J. (2001). Polysaccharide colloidal particles as delivery systems for macromolecules. *Advanced Drug Delivery Reviews*, *47*, 83–97.

Ji, Q. X., Zhong, D. Y., Lu, R., Zhang, W. Q., Deng, J., & Chen, X. G. (2009). In vitro evaluation of the biomedical properties of chitosan and quaternized chitosan for dental applications. *Carbohydrate Research*, *344*, 1297–1302.

Juergensen, L., Busnarda, J., Caux, P. Y., & Kent, R. A. (2000). Fate, behavior, and aquatic toxicity of the fungicide DDAC in the Canadian environment. *Environmental Toxicology*, *15*, 174–200.

Kastner, U., Hoffmann, H., Donges, R., & Ehrler, R. (1996). Interactions between modified hydroxyethyl cellulose (HEC) and surfactants. *Colloids and Surfaces A*, *112*, 209.

Langevin, D. (2009). Complexation of oppositely charged polyelectrolytes and surfactants in aqueous solutions. A review. *Advances in Colloid and Interface Science*, *147–148*, 170–177.

Lapitsky, Y., Parikh, M., & Kaler, E. W. (2007). Calorimetric determination of surfactant/polyelectrolyte binding isotherms. *Journal of Physical Chemistry B*, *111*, 8379–8387.

Lapitsky, Y., Zahir, T., & Shoichet, M. S. (2008). Modular biodegradable biomaterials from surfactant and polyelectrolyte mixtures. *Biomacromolecules*, *9*, 166–174.

Leong, K. W., Mao, H.-Q., Truong-Le, V. L., Roy, K., Walsh, S. M., & August, J. T. (1998). DNA-polycation nanospheres as non-viral gene delivery vehicles. *Journal of Controlled Release*, *53*, 183–193.

Li, X. L., & Brownawell, B. J. (2010). Quaternary ammonium compounds in urban estuarine sediment environments – a class of contaminants in need of increased attention? *Environmental Science & Technology*, *44*, 7561–7568.

Lim, S. H., & Hudson, S. M. (2003). Review of chitosan and its derivatives as antimicrobial agents and their uses as textile chemicals. *Journal of Macromolecular Science: Polymer Reviews*, *C43*, 223–269.

Lim, S. H., & Hudson, S. M. (2004). Synthesis and antimicrobial activity of water-soluble chitosan derivative with a fiber-reactive group. *Carbohydrate Research*, *339*, 313–319.

Madihally, S. V., & Matthew, H. W. T. (1999). Porous chitosan scaffolds for tissue engineering. *Biomaterials*, *20*, 1133–1142.

Matulis, D., Rouzina, I., & Bloomfield, V. A. (2002). Thermodynamics of cationic lipid binding to DNA and DNA condensation: Roles of electrostatics and hydrophobicity. *Journal of the American Chemical Society*, *124*, 7331.

Morris, G. A., Castile, J., Smith, A., Adams, G. G., & Harding, S. E. (2011). The effect of prolonged storage at different temperatures on the particle size distribution of tripolyphosphate (TPP) – chitosan nanoparticles. *Carbohydrate Polymers*, *84*, 1430–1434.

Murata, H., Koepsel, R. R., Matyjaszewski, K., & Russell, A. J. (2007). Permanent, non-leaching antibacterial surfaces – 2: How high density cationic surfaces kill bacterial cells. *Biomaterials*, *28*, 4870–4879.

Muzzarelli, R. A. A. (2009). Chitins and chitosans for the repair of wounder skin, nerve, cartilage and bone. *Carbohydrate Polymers*, *76*, 167–182.
Nobbmann, U., & Morfesis, A. (2008). Characterization of nanoparticles by light scattering. *MRS Proceedings*, *1074*, 1074-I1010-1045
Ohbu, K., Hiraishi, O., & Kashiwa, I. (1982). Effect of quaternary ammonium substitution of hydroxyethylcellulose on binding of dodecyl-sulfate. *Journal of the American Oil Chemists Society*, *59*, 108.
Pepic, I., Filipovic-Grcic, J., & Jalsenjak, I. (2008). Interactions in a nonionic surfactant and chitosan mixtures. *Colloids and Surfaces A*, *327*, 95–102.
Pillai, C. K. S., Paul, W., & Sharma, C. P. (2009). Chitosan and chitosan polymers: Chemistry: Solubility and fiber formation. *Progress in Polymer Science*, *34*, 641–678.
Rasmusson, M., Routh, A., & Vincent, B. (2004). Flocculation of microgel particles with sodium chloride and sodium polystyrene sulfonate as a function of temperature. *Langmuir*, *20*, 3536–3542.
Rinaudo, M. (2006). Chitin and chitosan: Properties and applications. *Progress in Polymer Science*, *31*, 603–632.
Sandbacka, M., Christianson, I., & Isomaa, B. (2000). The acute toxicity of surfactants on fish cells, Daphnia magna and fish – A comparative study. *Toxicology in Vitro*, *14*, 61–68.
Shi, Z., Neoh, K. G., Kang, E. T., & Wang, W. (2006). Antibacterial and mechanical properties of bone cement impregnated with chitosan nanoparticles. *Biomaterials*, *27*, 2440–2449.
Smitha, B., Sridhar, S., & Khan, A. (2004). Polyelectrolyte complexes of chitosan and poly(acrylic acid) as proton exchange membranes for fuel cells. *Macromolecules*, *37*, 2233–2239.
Streletzky, K., & Phillies, G. D. J. (1995). Temperature dependence of Triton X-100 micelle size and hydration. *Langmuir*, *11*, 42–47.
Tashiro, T. (2001). Antibacterial and bacterium adsorbing macromolecules. *Macromolecular Materials and Engineering*, *286*, 63–87.
Thalberg, K., Lindman, B., & Bergfeldt, K. (1991). Phase behavior of systems of polyacrylate and cationic surfactants. *Langmuir*, *7*, 2893.
Thalberg, K., Lindman, B., & Karlstrom, G. (1991). Phase behavior of a system of cationic surfactant and anionic polyelectrolyte: The effect of salt. *Journal of Physical Chemistry*, *95*, 6004–6011.
Thurston-Enriquez, J. A., Haas, C. N., Jacangelo, J., & Gerba, C. P. (2003). Chlorine inactivation of adenovirus type 40 and feline calicivirus. *Applied and Environmental Microbiology*, *69*, 3979–3985.
Tsai, M. L., Chen, R. H., Bai, S. W., & Chen, W. Y. (2011). The storage stability of chitosan/tripolyphosphate nanoparticles in a phosphate buffer. *Carbohydrate Polymers*, *84*, 756–761.
Wang, X., Du, Y., Yang, J., Tang, Y., & Luo, J. (2008). Preparation, characterization, and antimicrobial activity of quaternized chitosan/organic montmorillonite nanocomposites. *Journal of Biomedical Materials Research Part A*, *84A*, 384–390.
Wang, Y. L., Kimura, K., Dubin, P. L., & Jaeger, W. (2000). Polyelectrolyte-micelle coacervation: Effects of micelle surface charge density, polymer molecular weight, and polymer/surfactant ratio. *Macromolecules*, *33*, 3324.
Wang, Y. L., Kimura, K., Huang, Q., Dubin, P. L., & Jaeger, W. (1999). Effects of salt on polyelectrolyte-micelle coacervation. *Macromolecules*, *32*, 7128.
Wu, J. Z., Huang, G., & Hu, Z. B. (2003). Interparticle potential and the phase behavior of temperature-sensitive microgel dispersions. *Macromolecules*, *36*, 440–448.
Zhang, H., Mardyani, S., Chan, W. C. W., & Kumacheva, E. (2006). Design of biocompatible chitosan microgels for targeted pH-mediated intracellular release of cancer therapeutics. *Biomacromolecules*, *7*, 1568–1572.